Computers & Fluids, Vol. 1, pp. 399–417. Pergamon Press. 1973, Printed in Great Britain

A TEST PARTICLE MONTE CARLO METHOD

THOMAS W. TUER* and GEORGE S. SPRINGER
Fluid Dynamics Laboratory, Department of Mechanical Engineering
The University of Michigan, Ann Arbor, Michigan, 48104, U.S.A.

(*Received* 14 *March* 1973)

Summary—A Monte Carlo technique was developed suitable for investigating rarefied gas dynamics problems. The procedure is based on the 'test particle' method. The discontinuous function frequently employed for describing the target molecules' velocity distribution is replaced here by a continuous analytic function, the form of which is prescribed prior to the calculations. This modification simplifies the calculations, reduces the computer storage requirements, and facilitates the application of the method to multi-dimensional problems. The accuracy and versatility of the technique was evaluated by obtaining solutions to several one dimensional problems for which other results exist.

1. INTRODUCTION

It is recognized that many complex rarefied gas dynamics problems, for which solutions cannot be obtained by analytical means, are amenable to Monte Carlo methods. The complexity of geometry and flow, and the degree of accuracy attainable by such methods are limited only by computer time and storage requirements. It is desirable, therefore, to reduce both these requirements without affecting the accuracy of the results. The Monte Carlo technique developed in this investigation was directed towards these goals.

The present technique is based on the 'test particle' method. In this method the progress of a test particle is followed through a field of target molecules. Generally, the target molecules' velocity distribution has been described by a discontinuous function determined completely within the calculation (e.g., see refs. 1–3). In the present investigation the target molecules' velocity distribution is specified prior to the calculations and only the constants in the functions are adjusted as the calculation progresses. The usefulness and accuracy of this procedure were evaluated by obtaining solutions to several problems, and by comparing these solutions to existing analytical, numerical and experimental results. In this paper, solutions to five different one-dimensional problems are discussed (Section 3). It is noted, however, that the problem of the expansion of a gas from an axisymmetric nozzle into a vacuum was also investigated[4].

2. DESCRIPTION OF THE MONTE CARLO TECHNIQUE

The following Monte Carlo procedure can be applied to problems involving the steady flow of a rarefied, electrically neutral, non-reacting, single specie gas. All intermolecular collisions are considered to be elastic, and the molecules are assumed to interact according to Maxwell's inverse fifth-power force law. However, the technique could readily be extended to include any inverse power law for binary collisions. The major steps of the technique for

* Present address: Science Applications, Inc., Ann Arbor, Michigan.

one 'iteration' are outlined below. This prodedure is repeated until the desired degree of convergence is attained. In principle, the method can be applied to one, two or three dimensional problems. However, in each case the success of the procedure depends on one's ability to select, prior to the calculations, a sufficiently accurate form of the target molecules' velocity distribution function (see Section 2.9). All equations presented below are for a cartesian coordinate system. Further details of these equations, including their derivations as well as their forms in cylindrical and spherical coordinate systems, are given in [4].

2.1 *Control volume and cells*

A finite region of the flow field to be studied is selected. This region, referred to as the 'control volume,' may be of any regular or irregular shape, with its boundaries along a solid wall or along an imaginary surface in the gas. The appropriate boundary conditions must be known along the entire surface of the control volume. When the boundary is a solid wall, the velocity and temperature of the surface and the parameters describing the gas-surface interaction must be known at every point. When the boundary is an imaginary surface in the gas, in general, the following parameters must be specified: the molecular number flux across the surface, the mean flow velocity (three components), and the kinetic temperature (three components) of the gas at this surface.

The control volume is subdivided into 'cells' of arbitrary shapes and sizes.

2.2 *Initial estimates in the cells*

In each cell, an initial estimate is made of the number density, the mean flow velocity, and the kinetic temperature of the gas. These parameters are assumed to be uniform in each cell and are not changed until the next iteration.

2.3 *Initial location of test particle*

A point on the boundary of the control volume is selected where the test particle is introduced into the control volume. For a closed control volume (i.e., gas is completely surrounded by solid boundaries) the initiation procedure is performed only once per iteration, and the point of initiation may be chosen arbitrarily. For an open control volume (i.e. gas may flow through at least part of the boundary) each time the test particle leaves the control volume it is re-introduced at an appropriate point along the control volume boundary. To accomplish this, the open boundary is subdivided into 'entrance faces' which may coincide with the cell boundaries (Fig. 1a), or may be smaller than the cell boundary (Fig. 1b). During any given iteration the number of test particles introduced through a given face is

$$\dot{N} = (G)(\dot{n}) \qquad (G > 0) \tag{1}$$

where G is an arbitrary proportionality factor, and $\dot{n}$ is the number of molecules which would actually pass through the face ($\dot{n}$ is given by the boundary conditions).

The point of initiation on the entrance face is selected randomly. For a two dimensional face in a cartesian coordinate system the coordinates of the starting point are

$$X_1 = R\,\Delta X_1 \qquad X_2 = R\,\Delta X_2 \tag{2}$$

X_1 and X_2 represent any two of the coordinates x, y, or z (depending on the orientation of the face), and ΔX_1 and ΔX_2 are the corresponding dimensions of the face (Fig. 1c). The R's are independent random deviates of a uniform distribution between zero and one. R may be generated by the IBM subroutine (RANDU). Each time R appears it is a new random number.

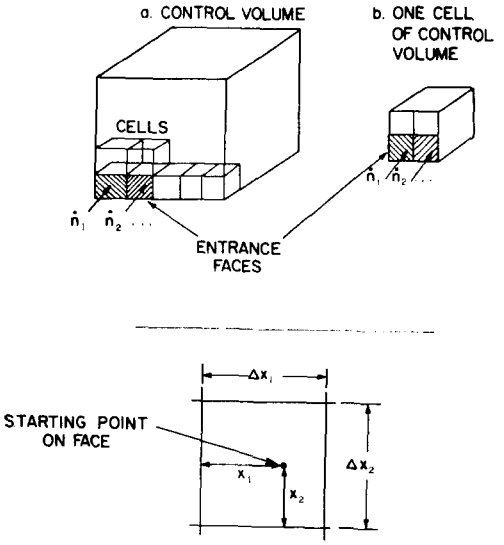

Fig. 1. Upper figures, control volume, cells and entrance faces in Cartesian coordinates; lower figure, coordinates of the starting point on an entrance face in Cartesian coordinate system.

2.4 *Test particle's initial velocity*

Once the location for initiating the test particle is determined, the initial velocity of the test particle is selected statistically. For a closed control volume the initial velocity need be selected only once, and any non-zero velocity may be used. At the boundary of an open control volume the initial velocity of the test particle may be obtained from the formulae given below. These formulae are based on the assumption of local equilibrium at the boundary. The velocity component normal to the boundary (u_1) is[1]

$$u_1 = \sqrt{2\hat{R}T_b}\,\Omega(U, R) \tag{3}$$

$\Omega(U, R)$ is the positive root of the equation:

$$R = \frac{\exp[-(U-\Omega)^2] + \pi^{1/2}U[1 + \operatorname{erf}(U-\Omega)]}{\exp(-U^2) + \pi^{1/2}U(1 + \operatorname{erf} U)} \tag{4}$$

and

$$U \equiv \bar{u}_1/(2\hat{R}T_b)^{1/2}. \tag{5}$$

$\hat{R}$ is the gas constant per unit mass, and T_b is the temperature of the boundary. The velocity components of the test particle tangent to the boundary are

$$u_{2,3} = \left(\frac{12\hat{R}T_b}{M}\right)^{1/2}\left(\sum_{k=1}^{M} R_k - \frac{M}{2}\right) + \bar{u}_{2,3} \tag{6}$$

where M is some large integer usually taken as 12 [5]. The components of the mean flow velocity of the gas ($\bar{u}_1$, $\bar{u}_2$, $\bar{u}_3$) are given by the boundary conditions.

Similar expressions are not available when the gas cannot be taken to be in local equilibrium at the boundary. In this case, u_1, u_2, and u_3 may be approximated by replacing T_b in equation (5) by T_1, and in equation (6) by T_2 and T_3, where T_1, T_2, T_3 are the components of the kinetic temperature of the gas in the direction of u_1, u_2, and u_3, respectively.

2.5 *Time to cell crossing*

The time τ_B is calculated, where τ_B is the time required for the test particle to travel from its present location (A) to the boundary of the cell (B), if it does not experience a collision between A and B. Point A may be either on the surface of the cell (Fig. 2a) or within the

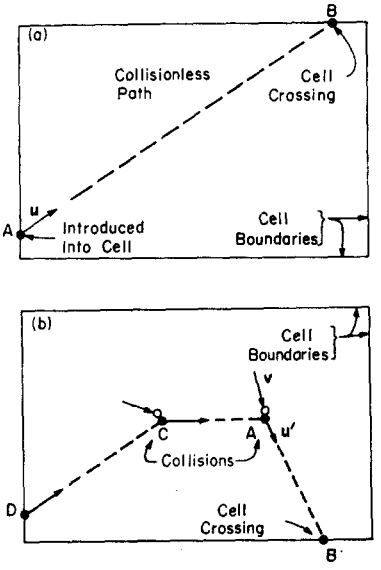

Fig. 2. Schematics of typical test particle trajectories in a cell; (a) no collisions, (b) with collisions.

cell. In the latter case, point A is the position where the test particle encountered its last collision (Fig. 2b). The time required for a particle to cross the boundary of a cell is

$$\tau_B = \frac{\overline{AB}}{|\mathbf{u}_B|} \tag{7}$$

$\mathbf{u}_B$ is the test particle's velocity, and $\overline{AB}$ the distance between points A and B.

2.6 *Time to collision*

The time τ_c is evaluated, where τ_c is the time the test particle spends either between two collisions (path CA, Fig. 2b), or between entering the cell and its first collision in that cell (path DC). τ_c is selected from the expression [1]

$$\tau_c = \frac{1}{Z} \ln R$$

Z is the collision rate between the test particle and the surrounding molecules (target molecules). For molecules obeying Maxwell's inverse fifth power force law, Z may be expressed as

$$Z = \pi n V_{0_{\max}}^2 \left(\frac{2\kappa}{m}\right)^{1/2} \tag{9}$$

In equation (9) n is the number density in the cell (based on the estimate made prior to the beginning of the iteration), $V_{0_{max}}$ is a constant which, for Maxwellian molecules, is approximately equal to 1·5[1], κ is the coefficient in the inter-molecular force law, and m is the molecular mass.

2.7 *Compare τ_B and τ_c*

In order to determine if the test particle actually experiences a collision in the cell, the magnitudes of τ_B and τ_c are compared. When τ_B is smaller than τ_c, the test particle is considered to escape from the cell without suffering a collision (Section 2.8). When τ_c is smaller than τ_B, the test particle is assumed to collide with a target molecule before leaving the cell (Section 2.9).

2.8 *Cell crossing event*

When τ_B is smaller than τ_c the test particle is assumed to reach the boundary of the cell before experiencing another collision (Point B, Fig. 2). In this case one must calculate the coordinates of the point where the test particle leaves the cell and the test particle's velocity $\mathbf{u}_B$ at this point. In a cartesian coordinate system the coordinates of the exit point are

$$x_B = x_A + \tau_B u_{Bx},\ y_B = y_A + \tau_B u_{By},\ z_B = z_A + \tau_B u_{Bz}. \tag{10}$$

The subscript A refers to the coordinates of the starting point of the test particle (Point A, Fig. 2). u_{Bx}, u_{By} and u_{Bz} are the velocity components of the test molecules between points A and B, which, in a cartesian coordinate system, remain unchanged between points A and B. Once $\mathbf{u}_B$ is known certain products of τ_B and $\mathbf{u}_B$ are recorded for this cell, as described in Section 2.10.

After the coordinates of point B are determined, the test particle is 'moved' to this point and the boundary is checked to see whether or not it is also a control volume boundary. When the cell boundary is not a control volume boundary the test particle is assumed to enter the adjacent cell. When the cell boundary is also an imaginary boundary of the control volume the test particle is lost from the control volume, and we return to Section 2.4. When the boundary is a solid wall at the point of impact the test particle is assumed to rebound back into the control volume. The gas-surface interaction at the wall may be described by accommodation coefficients. Here the Maxwell accommodation coefficient F is used to calculate the test particle's velocity after a collision with the wall. F is the fraction of the molecules which impinges on the wall and emerges with a Maxwellian distribution characteristic of the wall temperature, and $(1-F)$ is the fraction which is specularly reflected. Prior to the calculations a value of F is selected based on the gas and the surface. Then, at each wall collision a random number R is generated and compared with F. When $R > F$, the collision is taken to be specular, and when $R < F$ it is taken to be diffuse. For specular reflections the components of the test particle's velocity tangential to the wall remain unchanged while the sign of the normal component is simply reversed. For diffuse reflections totally new velocity components are generated for the test particle using the equations

$$u_1 = u_{b_1} \pm \sqrt{2\hat{R}T_b}(\ln R)^{1/2} \tag{11a}$$

$$u_{2,3} = u_{b_{2,3}} + \sqrt{\frac{12\hat{R}T_b}{M}}\left(\sum_{k=1}^{M} R_k - \frac{M}{2}\right) \tag{11b}$$

u_{b_1}, u_{b_2} and u_{b_3} are the velocity components of the wall (for a stationary wall: $u_{b_1} = u_{b_2} = u_{b_3} = 0$). In equation (11a) the positive sign is used when the outward normal to the wall is in the positive u_1 direction. After calculating these velocity components we return to Section 2.5.

2.9 *Inter-molecular collision*

When τ_c is smaller than τ_B the test particle is assumed to collide with another molecule before leaving the cell. The coordinates of the collision point are

$$x_c = x_s + \tau_c u_{c_x},\ y_c = y_s + \tau_c u_{c_y},\ z_c = z_s + \tau_c u_{c_z} \tag{12}$$

The subscript s refers to the point where the last event occured prior to the collision (i.e. either point D or C in Fig. 2*b*). $\mathbf{u}_c$ is the test particle's velocity just before the collision and is identical to its velocity at either point D or point C in Fig. 2b. Certain products of τ_c and $\mathbf{u}_c$ are formed then, as explained in Section 2.10.

After the location of the collision and the velocity of the test particle $\mathbf{u}_c$ have been determined, the test particle is moved to the site of collision (points C or A, Fig. 2) and the velocity $\mathbf{v}$ of the collision partner (target molecule) is selected. In selecting $\mathbf{v}$ it is assumed that the target molecules' distribution function in the cell can be expressed as:

$$f(\mathbf{v}) = f_x(v_x) f_y(v_y) f_z(v_z) \tag{13}$$

and

$$f_i(v_i) = (2\pi \hat{R} T_i)^{-1/2} \exp\left[-\frac{(v_i - \bar{u}_i)^2}{2\hat{R}T_i}\right] \tag{14}$$

where u_i is the i the component of the mean flow velocity and T_i the component of the kinetic temperature of the gas in the cell ($i = x, y, z$). It must be emphasized that the above distribution function applies only to the target molecules, and is only used to select statistically the collision partners' velocities. No restriction is made regarding the test particles' distribution function.

With the above assumptions, and for molecules interacting according to Maxwell's inverse fifth power force law, the velocity components of the collision partner (target molecule) before collision are

$$v_i = \bar{u}_i + \left(\frac{12\hat{R}T_i}{M}\right)^{1/2} \left(\sum_{k=1}^{M} R_k - \frac{M}{2}\right). \tag{15}$$

The velocity components of the test particle after collision are calculated from the expressions[6]

$$\begin{aligned} u_x' &= u_x + (w_y^2 + w_z^2)^{1/2} \sin\varepsilon \cos\psi \sin\psi - w_x \cos^2\psi \\ u_{y,z}' &= u_{y,z} - (\mp w w_{z,y} \cos\varepsilon - w_x w_{y,z} \sin\varepsilon) \\ &\quad \cdot (w_y^2 + w_z^2)^{-1/2} \cos\psi \sin\psi - w_{y,z} \cos^2\psi. \end{aligned} \tag{16}$$

The relative velocity components are defined as

$$w_i \equiv u_i - v_i, \qquad w^2 = w_x^2 + w_y^2 + w_z^2. \tag{17}$$

The collision parameters ε and ψ are statistically selected using [1]:

$$\varepsilon = 2\pi R, \qquad \psi = \left[1 + \frac{2}{(V_{0_{max}} R)^4}\right]^{-1/4} \omega(\eta) \tag{18}$$

where ω is an elliptic integral of the first kind, and

$$\eta \equiv \frac{1}{2}\left\{1 - \left[1 + \frac{2}{(V_{0_{max}} R)^4}\right]^{-1/2}\right\} \tag{19}$$

2.10 *Gas properties from statistical information*

After a pre-set number of collisions or cell crossings have been considered the flow parameters of interest in each cell are calculated. These calculations are based on the information accumulated in Sections 2.8 and 2.9, and are of the form of time weighted averages in each cell

$$\bar{Q} = \left[\sum_{q=1}^{N} Q_q \tau_q\right] \Big/ \left[\sum_{q=1}^{N} \tau_q\right] \tag{20}$$

τ_q is the time of travel in this cell (τ_B or τ_c) at a constant velocity ($\mathbf{u}_B$ or $\mathbf{u}_c$), and N is the total number of events (collision or boundary crossing) which occured in this cell. The quantities $(Q_q \tau_q)$ and τ_q are calculated for each event, but only the sum given by equation (20) is stored. For example, the ith component of the mean velocity is

$$\bar{u}_i = \left[\sum_{q=1}^{N} \tau_q u_{iq}\right] \Big/ \left[\sum_{q=1}^{N} \tau_q\right] \tag{21}$$

Other flow parameters of interest may be calculated in a similar manner. The number, momentum and energy fluxes in the i direction are

$$n\bar{u}_i = n\left[\sum_{q=1}^{N} \tau_q u_{iq}\right] \Big/ \left[\sum_{q=1}^{N} \tau_q\right] \tag{22a}$$

$$\overline{mu_i u_j} = m\left[\sum_{q=1}^{N} \tau_q u_{iq} u_{jq}\right] \Big/ \left[\sum_{q=1}^{N} \tau_q\right] \tag{22b}$$

$$\frac{m}{2}\overline{u_i(u_x^2 + u_y^2 + u_z^2)} = \frac{m}{2}\left[\sum_{q=1}^{N} u_{iq}(u_{xq}^2 + u_{yq}^2 + u_{zq}^2)\right] \Big/ \left[\sum_{q=1}^{N} \tau_q\right] \tag{22c}$$

The ith component of the kinetic temperature is

$$T_i = \frac{\overline{u_i^2} - \bar{u}_i^2}{n\hat{R}} = \frac{1}{n\hat{R}}\left\{\left[\sum_{q=1}^{N} \tau_q u_{iq}^2\right] \Big/ \sum_{q=1}^{N} \tau_q - \left[\sum_{q=1}^{N} \tau_q u_{iq}\right]^2 \Big/ \left[\sum_{q=1}^{N} \tau_q\right]^2\right\} \tag{23}$$

The number flux, momentum flux, energy flux, etc., crossing a boundary may be evaluated in an alternate manner by calculating the number, momentum, energy, etc., of all the test particles crossing the boundary.

The number density n in any cell is proportional to the time the test particle spends in this cell during an iteration (provided the cells are of equal volume). Thus, if the test particle spends time t_ℓ in the ℓth cell, then the density in this cell is

$$n_\ell = t_\ell \delta \tag{24}$$

The proportionality constant δ is determined either from the density known in one of the cells, or from the known average density in the entire control volume.

2.11 *Comparison with Haviland's Monte Carlo procedure*

The technique described above is along the lines suggested by Haviland[1]. However, there are some significant differences between the two methods, namely in the respective techniques employed for storing information about the target molecules' and the test particle's velocity distribution functions. In Haviland's method two separate sets of velocity compartments are established in each physical cell. The target molecules' velocity distribution function is stored in one of these sets by specifying the number of molecules whose velocities lie within the range of each velocity compartment. The second set of velocity compartments is utilized to store the test particle's velocity distribution function which is generated during the Monte Carlo procedure. This scheme requires a large number of compartments (i.e., computer storage). It also necessitates the selection of collision partners from a large number of discrete numbers which is a time consuming procedure on the computer. These difficulties are overcome in the present method by describing the target molecules' velocity distribution by a continuous analytic function (specified by only seven parameters, n, u_x, u_y, u_z, T_x, T_y and T_z), and by storing only moments of the test particle's velocity. These steps greatly reduce computing time and storage requirements.

In its present form the technique does not provide the test particle's velocity distribution function. Nevertheless, it yields with reasonable accuracy moments of the test particle's distribution function (e.g., density, mean flow velocities, kinetic temperatures, fluxes), which are the quantities of practical interest.

3. SAMPLE PROBLEMS

The Monte Carlo technique described in the previous section was applied to a number of problems for which other analytical, numerical, or experimental results exist. In accordance with the procedure established in Section 2, the calculations were performed assuming Maxwellian molecules.

3.1 *Gas at equilibrium between parallel plates*

A gas at equilibrium, with uniform number density n is contained between two infinite parallel plates separated by a distance S and maintained at the same constant, uniform temperature T. The accommodation coefficients at both walls are unity ($F = 1$). By introducing the dimensionless parameters*

$$S^* = S/L_R;\ T^* = T/T_R;\ u^* = u/\sqrt{2\hat{R}T_R};\ n^* = nL_R{}^3 \tag{25}$$

and by setting the reference length L_R and reference temperature T_R equal to S and T, respectively, we obtain

$$S^* = 1;\ T^* = 1;\ n^* = 2{\cdot}18\,\frac{S}{\lambda} = \frac{2{\cdot}18}{Kn}. \tag{26}$$

* The same non-dimensional parameters are used also in the problems given in Sections 3·2–3·5.

In deriving n^*, the parameter

$$\kappa^* = (\kappa/m)(2\hat{R}T_R L_R{}^4)^{-1} \tag{27}$$

was taken to be 0·01402. This value, suggested by Haviland[1], was used also in all subsequent calculations. With the above non-dimensionalization the problem is defined by a single parameter, the Knudsen number ($Kn = \lambda/S$). The value $Kn = 1{\cdot}0$ was used to correspond to the value used in ref. 1.

The control volume included the entire region between the plates, and a single cell was used to cover the entire control volume. In every calculation the initial estimates (denoted by subscript 0) were: gas density $n_0{}^* = 2{\cdot}18$, mean gas velocity $\bar{u}_0{}^* = 0$, and gas temperature $T_0{}^* = 1$.

Computer calculations were made varying the number of inter-molecular collisions. The convergence of the second order moments (i.e., $\overline{u_x{}^2}$ and $\overline{u_t{}^2}$) toward the equilibrium value is shown in Fig. 3. As can be seen, after about 4000 inter-molecular collisions the results agree within about one per cent with the results of equilibrium theory.

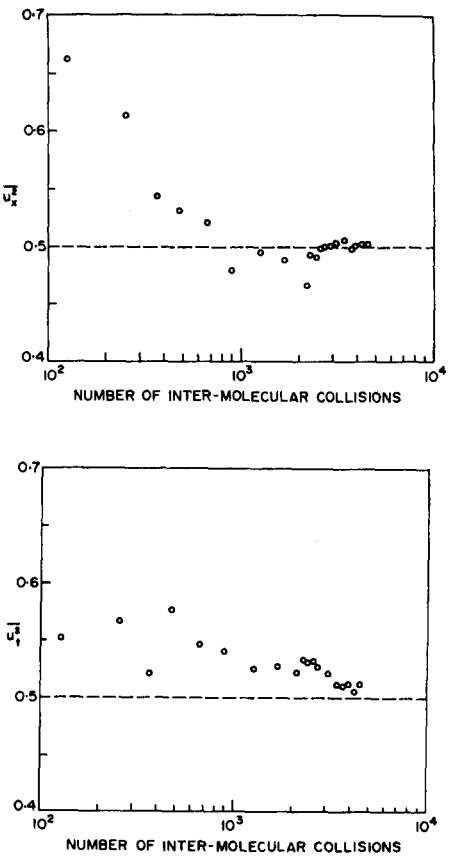

Fig. 3. Rarefied gas contained between isothermal parallel plates. Convergence of second order moments with number of inter-molecular collisions. ○ present results, ---- equilibrium theory.

Results after 895 collisions for these and other moments are compared to the results of Haviland[1] for the same conditions and a similar number of collisions in Table 1. The

Table 1. Rarefied gas contained between isothermal parallel plates. Comparison with Haviland's results and with equilibrium theory

Moment	Present	Haviland	Equilibrium theory
$\bar{u}_x$	6×10^{-9}	0·0463	0
$\overline{u_x^2}$	0·4796	0·4486	0·5
$\overline{u_t^2}$	0·5402	0·4912	0·5
$\overline{u_x^3}$	0·0528	0·1026	0
$\overline{u_x u_t^2}$	0·0296	0·0293	0
$\overline{u_x^4}$	0·6508	0·6552	0·75
$\overline{u_x^2 u_t^2}$	0·2419	0·2355	0·25
$\overline{u_t^4}$	0·8247	0·7118	0·75

present results are generally in somewhat better agreement with equilibrium theory than are those of Haviland. The higher order moment require that more collisions be considered than the lower moments for the same accuracy.

3.2 *Gas between parallel plates at different temperatures*

A rarefied gas is contained between two infinite parallel plates separated by a distance S. The average number density of the gas is $n = N_M/S$, where N_M is the total number of molecules between the plates per unit area of the plates. The plates are maintained at different uniform and constant temperatures, T_{I} and T_{II}. The accommodation coefficients at the walls are F_{I} and F_{II}. The parameters S, n, T_{I} and T_{II} may be related to the temperature ratio $T_{\mathrm{I}}/T_{\mathrm{II}}$ and the Knudsen number $\bar{K}n = \bar{\lambda}/S$, where $\bar{\lambda}$ is the average mean free path in the gas. Calculations were performed for different values of these parameters (Table 2). The control

Table 2. Boundary and initial conditions used in the calculations for a gas between parallel plates at unequal temperatures

	Case *A*	Case *B*
$T_{\mathrm{I}}/T_{\mathrm{II}}$	4	3·72
$\bar{K}n$	0·524	0·399, 0·118, 0·053
$F_{\mathrm{I}} = F_{\mathrm{II}}$	1	0·58
$n_0{}^*$	1	continuum theory
$\bar{u}_0{}^*$	0	0
$T_0{}^*$	1	1

volume included the entire region between the plates and was divided into ten cells of equal size.

Case A was considered in order to determine how many iterations were required before results became repeatable within acceptable limits and the amount of scatter typical in the

results. The initial estimates for the first run were considered uniform over the control volume (Table 2) since this was expected to require the most iterations before 'repeatability' was attained. A total of six runs were made with 20,000 events (i.e. intermolecular collisions or cell crossings) in each run. Density distributions calculated from the last three runs are shown in Fig. 4, indicating the scatter in the results. Eighty-seven per cent of the individual

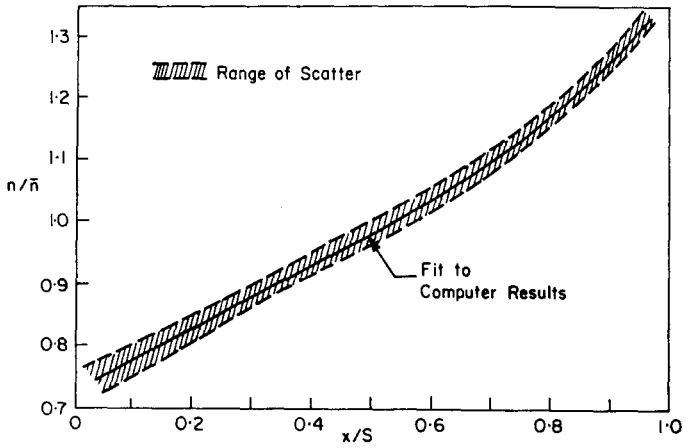

Fig. 4. Rarefied gas contained between parallel plates at different temperatures. Number density as a function of position normal to hot plate. ($T_I/T_{II} = 4$, $\bar{K}n = 0{\cdot}524$, $F_I = F_{II} = 1$).

data points calculated in these last three runs fell within the indicated scatter band. The 'best fit' to the last three runs is compared to analytical results of Liu and Lees[7] and Ziering[8], and to the Monte Carlo results of Haviland[1] (Fig. 5). General agreement is evident between all four calculations with the present results matching those of Ziering's best.

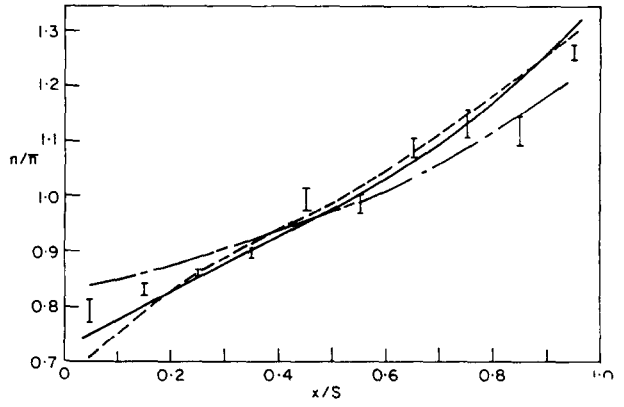

Fig. 5. Rarefied gas contained between parallel plates at different temperatures. Number density as a function of position normal to hot plate: ——— present method; —·— Lees and Liu[7]; ---- Ziering[8]; I Haviland[1]. ($T_I/T_{II} = 4$, $\bar{K}n = 0{\cdot}524$, $F_I = F_{II} = 1$).

Case B was considered in order to compare the density distributions calculated by the present method with the experimental data of Alofs and Springer[9], with the results of Liu and Lees' four moment method of solution of the Boltzmann equation[10], and with continuum theory[9] (Fig. 6). The present results are in good agreement both with the experimental measurements and with Liu-Lees' results.

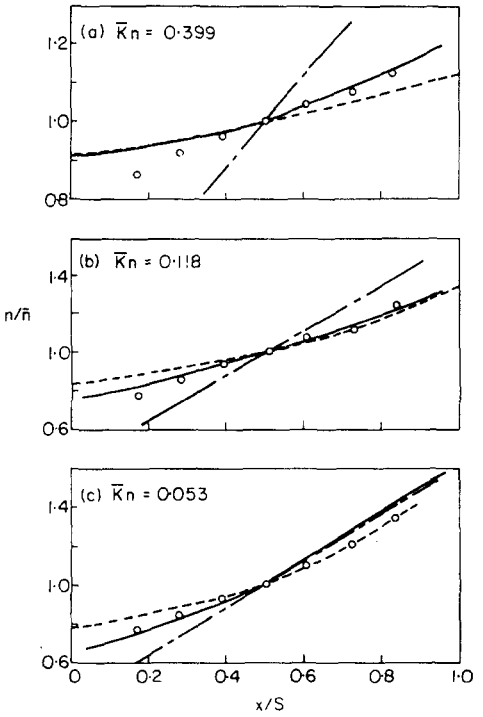

Fig. 6. Rarefied gas contained between parallel plates at different temperatures. Comparison of calculated and measured number densities: ——— present method; ---- Liu and Lees[10]; —·— continuum theory[9]; ○ Alofs and Springer's data[9]; as a function of position normal to hot plate. ($T_I/T_{II} = 3{\cdot}72$, $F_I = F_{II} = 0{\cdot}58$).

3.3 *Normal shock*

Consider a stationary normal shock in a rarefied gas. Far upstream from the shock ($x \to -\infty$) the gas is in local equilibrium with number density n_I, mean flow velocity normal to the shock $\bar{u}_{x_I}$, and equilibrium temperature T_I. Far downstream ($x \to +\infty$) the gas is equilibrated locally with density n_{II}, velocity $\bar{u}_{x_{II}}$ and temperature T_{II}. By selecting the reference length and temperature to be $L_R = \lambda_I$ and $T_R = T_I$, the foregoing parameters may be expressed in terms of a single parameter, the upstream Mach number Ma_I. In order to compare the present results with existing solutions[11, 12], we used $Ma_I = 8$.

The control volume was divided into 36 cells and extended far enough upstream and downstream so that the gas at these boundaries was nearly in equilibrium. The calculations presented are for the boundary positions: $x_I^* = x_I/\lambda_I = -9{\cdot}47$ and $x_{II}^* = x_{II}/\lambda_I = 9{\cdot}47$.

For the first run, in each cell the initial estimates of density was based on the Mott–Smith expression[13]:

$$n_0^* = n_{II}^* + (n_I^* - n_{II}^*)/[1 + \exp(4x^*/W^*)] \tag{28}$$

The shock thickness was taken to be $W^* = 7{\cdot}7$, as suggested by Bird[11] for $Ma_I = 8$. Initial estimates of the mean flow velocity and temperature were

$$\bar{u}_{x_0}^* = \bar{u}_{y_I}^* n_I^*/n_0^* \qquad \bar{u}_{y_0}^* = \bar{u}_{z_0} = 0 \tag{29}$$

$$T_{x_0}^* = T_{y_0}^* = T_{z_0}^* = T_I^* + (T_{II}^* - T_I^*)\frac{\bar{u}_{xII}^{*2} - \bar{u}_{x_0}^{*2}}{\bar{u}_{xII}^{*2} - \bar{u}_{xI}^{*2}} \tag{30}$$

About ten iterations, each considering 40,000 events, were required to attain acceptable repeatability and scatter in the results. The density, mean flow velocity and the normal and tangential components of the kinetic temperature calculated from the last five iterations, are shown in Figs. 7, 8. These figures indicate the scatter associated with the procedure. The

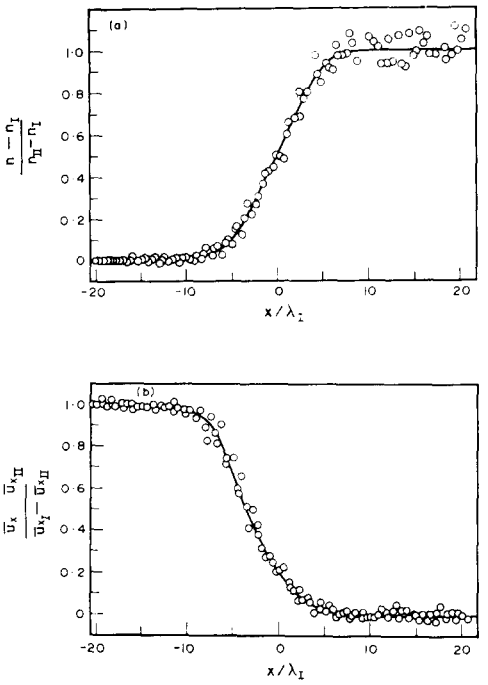

Fig. 7. Normal shock, (a) number density and (b) mean flow velocity normal to shock. ○ present computer results; ——— fit to computer results. ($Ma_I = 8$).

characteristic overshoot in T_x is evident in these results. A comparison was also made between the smoothed results of the density calculations and the results of the Monte Carlo calculations of Bird[11] and Yen[12] (Fig. 9). The results of all three of these methods are in reasonable agreement. The present results are closer to those of Yen downstream, but somewhat closer to those of Bird upstream.

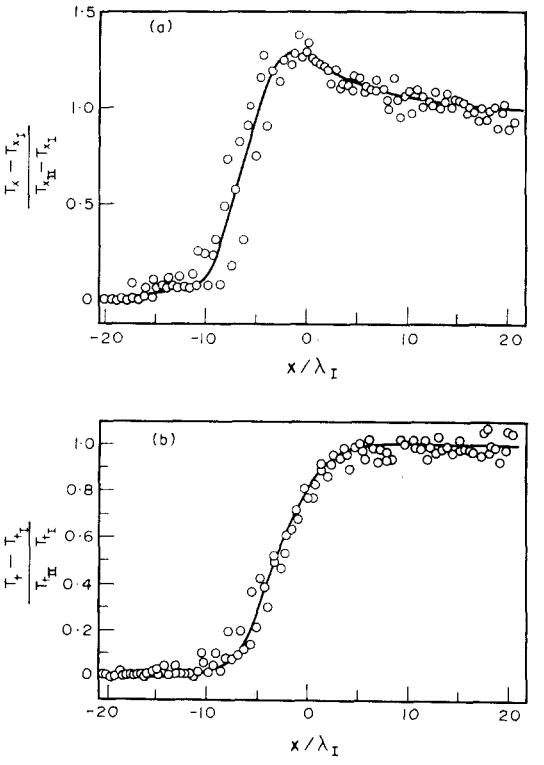

Fig. 8. Distribution of the kinetic temperatures through a normal shock, component (a) normal and (b) tangent to shock: ○ present computer results; ——— fit to computer results. ($Ma_I = 8$).

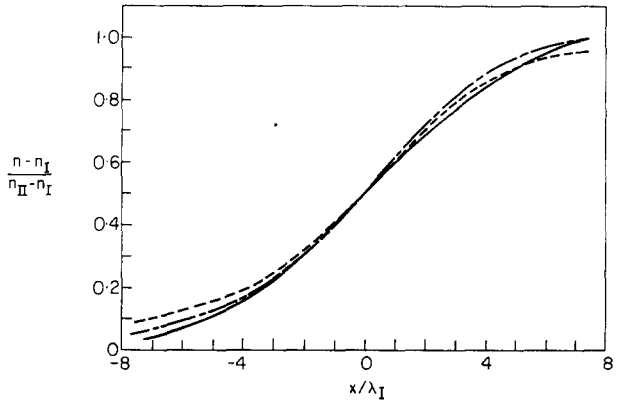

Fig. 9. Number density distributions through normal shock, comparison of various Monte Carlo results: ——— present method; —·— Bird[11]; ···· Yen[12]. ($Ma_I = 8$).

3.4 *Spherical source flow*

Consider the steady, spherical expansion of a gas from a point source into a vacuum (Fig. 10). At some distance from the source r_s the flow changes from subsonic to supersonic. The stagnation values of molecular number density and temperature at the source are n_T and T_T, respectively. Although these quantities are required as inputs to the Monte Carlo

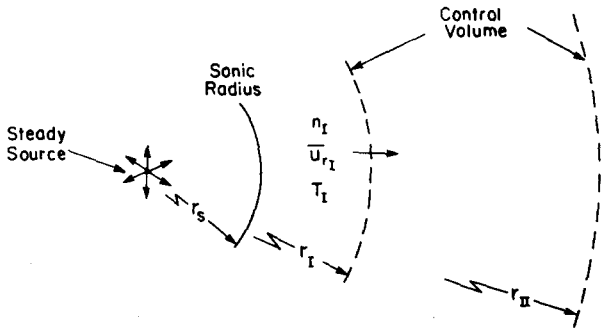

Fig. 10. Notation used in the spherical and cylindrical source flow problems.

calculation, the problem may be specified in terms of a single non-dimensional parameter, the source Knudsen number $Kn_T = \lambda_T/r_s$, where λ_T is the mean free path of the gas corresponding to the source density and temperature. Knowing the source Knudsen number, the reference length ($L_R = r_s$) and the reference temperature ($T_R = T_T$), the quantities n_T^*, T_T^* and r_s^*, can be evaluated readily. The Knudsen number used in the present calculations was selected to correspond to the value used by Bird[14] ($Kn_T = 0{\cdot}002$). The control volume was also selected to correspond to the region investigated by Bird[14], and included the region between two concentric spheres of radii: $r_I^* = r_I/r_s = 3$ and $r_{II}^* = r_{II}/r_s = 60$. The inner boundary ($r_I^*$) was close enough to the source so that the gas there could be assumed to be in local equilibrium. The control volume was divided into 40 cells in the form of concentric spherical shells of equal thickness. Initial estimates of density, velocity and temperature were based on isentropic theory[15].

The density, the mean flow velocity in the radial direction, and the radial and tangential components of kinetic temperature were calculated, all as a function of distance from the source r/r_s (Figs. 11, 12). Five iterations were made, each with 20,000 events, and the results of the last three iterations are shown in Figs. 11, 12. For the density, only the results of the third iteration are shown since these are essentially the same as those of the subsequent iterations. The density and the mean flow velocity obtained here are in good agreement with

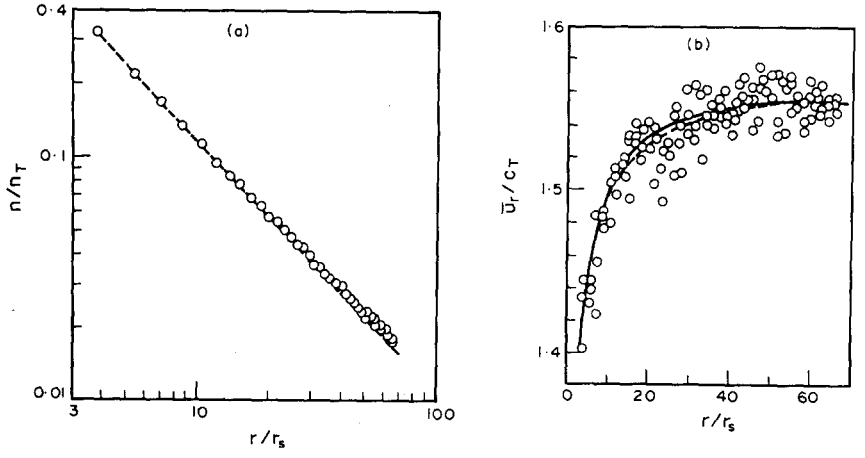

Fig. 11. Spherical source flow, (a) number density and (b) mean radial flow velocity: ○ present computer results; ——— fit to computer results; ---- isentropic theory. ($Kn_T = 0{\cdot}002$).

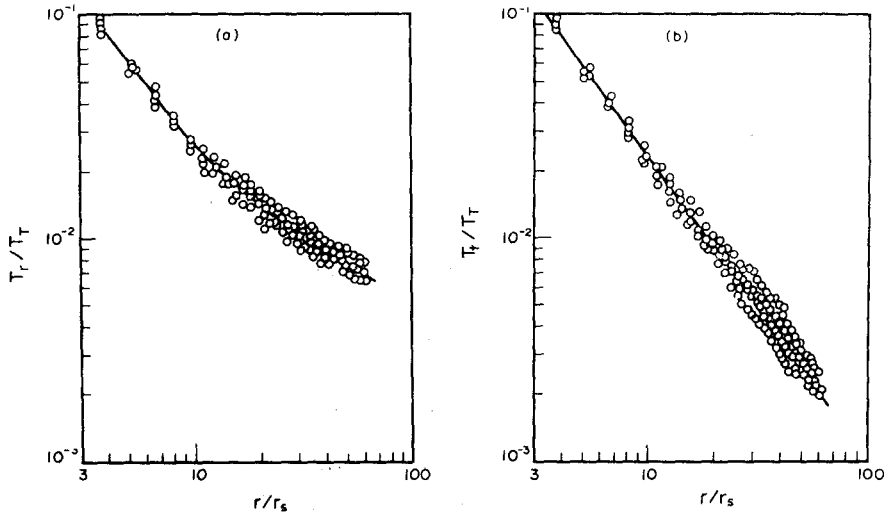

Fig. 12. Spherical source flow, kinetic temperatures as a function of distance from the source. (a) radial component and (b) transverse component: ○ present computer results; ——— fit to computer results; ---- isentropic theory. ($Kn_T = 0{\cdot}002$).

the results of isentropic theory (Fig. 11). Because the velocity scale is expanded in Fig. 11, the scatter appears to be worse than it actually is. The components of the kinetic temperatures are given in Fig. 12. In Fig. 13, the best fit to the radial component of kinetic temperature is compared to the results of Bird's Monte Carlo calculations[14], to analytical results

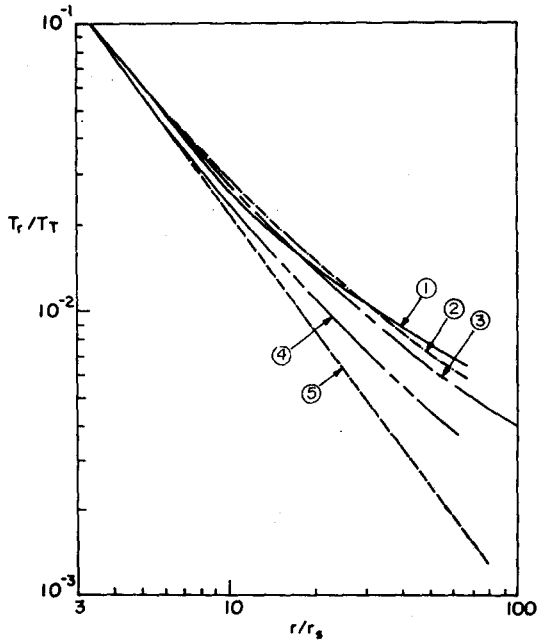

Fig. 13. Spherical source flow, radial component of kinetic temperature as a function of distance from source. Comparison of various results: (1) present results; (2) Soga and Oguchi[16]; (3) Bird[13]; (3) Hamel and Willis[17]; (5) Isentropic theory. ($Kn_T = 0{\cdot}002$).

of Soga and Oguchi[16] and of Hamel and Willis[17], and to the results of the isentropic theory[15]. The present results are in good agreement with those of Bird, and Soga and Oguchi, while the results of Hamel and Willis are somewhat low. A similar comparison for the tangential components of kinetic temperature is not shown, since all results essentially agree with those given by the isentropic theory.

3.5 *Cylindrical source flow*

The problem of cylindrical source flow is very similar to the problem of spherical source flow discussed above. The most notable difference between the two problems is that in cylindrical source flow the gas expands into vacuum from a line source rather than from a point source. Thus, in cylindrical source flow the radial, axial and the asimuthal components of the kinetic temperature and test particle velocity must be calculated. The Knudsen number selected for the calculations corresponded to the value used by Bird[14] in his calculations of this problem ($Kn_T = 0{\cdot}005$). Nevertheless, a direct comparison between the present and Bird's results is not possible because Bird's solutions were for hard sphere molecules. The control volume was also chosen to coincide with the region Bird investigated, and extended from $r_I^* = r_I/r_s = 3$ to $r_{II}^* = r_{II}/r_s = 66{\cdot}3$. The control volume was divided into 40 cells in the form of concentric cylindrical annuli of equal thickness. The results of isentropic theory were used as initial estimates. Three iterations, each considering 40,000 events, were required to obtain adequate repeatability and scatter in the results (Figs. 14, 15).

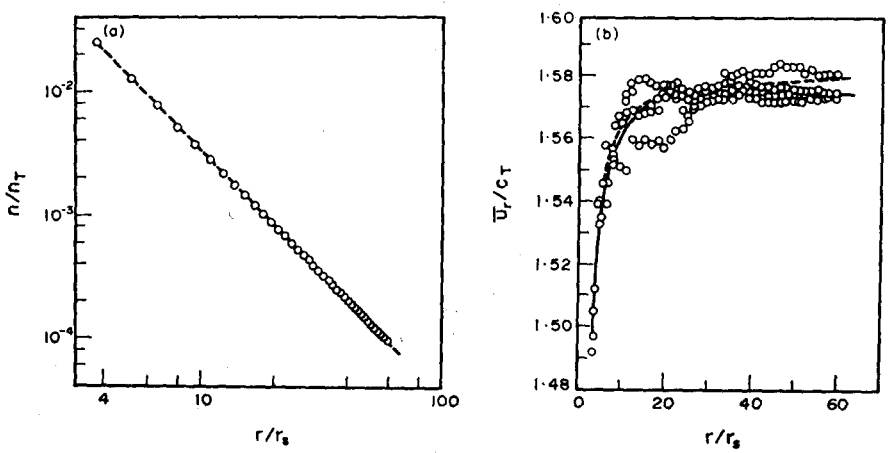

Fig. 14. Cylindrical source flow, (a) number density and (b) mean radial flow velocity: ○ present computer results; ——— fit to computer results; ---- isentropic theory. ($Kn_T = 0{\cdot}005$).

Similarly as in the spherical source flow problem, the density results of the first iteration (which are essentially the same as those of the latter iterations) and the mean flow velocity are in good agreement with the results of isentropic theory (Fig. 14). Note again the expanded scale. The components of kinetic temperature also follow closely the results given by the isentropic theory (Fig. 15). This is in agreement with Bird's observation[14] that for Maxwellian molecules in cylindrical source flow the kinetic temperature should not deviate from its isentropic value.

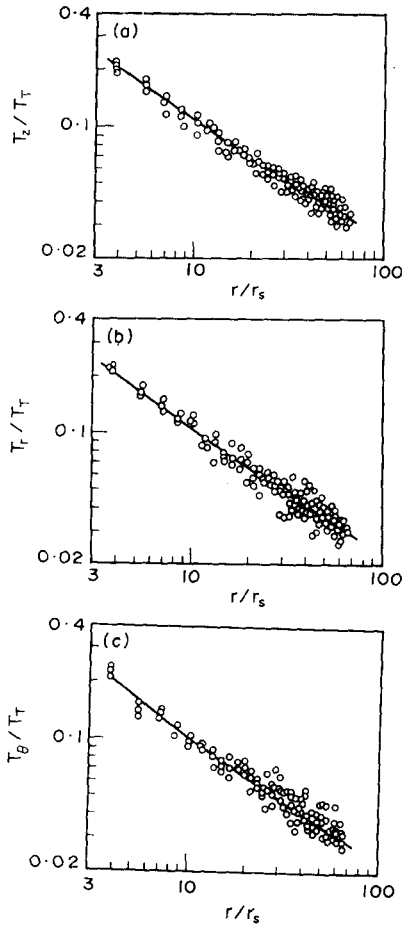

Fig. 15. Cylindrical source flow, kinetic temperatures as a function of distance from source, (a) axial, (b) radial and (c) azimuthal component: ○ present results; ——— fit to computer results. ($Kn_T = 0{\cdot}005$).

3.6 *Computer storage and running times*

Typical computer storage requirements for the sample problems considered in this section are presented in Table 3. The storage of other Monte Carlo methods are also given. Caution must be exercised in making direct comparisons between the various storage requirements because different investigators employed different computers, and sometimes determined quantities in addition to those calculated here. However, it appears that the present technique provides savings in storage over existing methods, at least for the calculation of the primary quantities of interest, such as density, mean flow, velocities and kinetic temperatures.

It would also be desirable to make comparisons of computer running times needed by the various methods. Unfortunately, the computer times required for the solution of the problems by the different methods cannot be assessed readily, because various investigators used

different computers, initial conditions and sample sizes (number of collisions) in their calculations.

Table 3. Comparison of computer storage requirements for various Monte Carlo methods

Problem	Method	Machine	Storage* (words)
Parallel plates at unequal temperatures	Haviland[1]	IBM 709	10^4
	Nordsieck[18]	Modern	—
	Present	IBM 360-67	80
Normal shock structure	Haviland[1]	IBM 709	10^4
	Bird[11]	IBM 360-75	10^4
	Nordsieck[19]	CDC 1604	—
	Present	IBM 360-67	324
Spherical source flow	Bird[14]	IBM 360-75	10^4
	Present	IBM 360-67	360
Cylindrical source flow	Bird[14]	IBM 360-75	10^4
	Present	IBM 360-67	600

* Not including instructions

Acknowledgment—The authors wish to thank Professor G. A. Bird for his helpful comments on the manuscript. This work was supported by the McDonnell-Douglas Astronautics Company.

REFERENCES

1. J. K. Haviland, The solution of two molecular flow problems by the Monte Carlo method, *Methods in Computational Physics* B. Alder, ed. **4**, 109–209. Academic Press, New York (1965).
2. A. W. Starr, Monte Carlo simulation of the flow of a rarefied gas around a cylinder, M.I.T. Lincoln Laboratory Technical Note 1967 (1967).
3. M. N. Kogan, Recent developments in the kinetic theory of gases, *Rarefied Gas Dynamics*, L. Trilling and H. Y. Wachman, ed. **1**, 1–39. Academic Press, New York (1969).
4. T. W. Tuer, A test particle Monte Carlo method with application to the free jet expansion problem, Ph.D. Thesis, The University of Michigan (1973).
5. R. W. Hamming, *Numerical Methods for Scientists and Engineers*, McGraw-Hill, New York (1962).
6. G. N. Patterson, *Molecular Flow of Gases*, Wiley, New York (1956).
7. L. Lees and C. Y. Liu, Kinetic theory description of plane compressible couette flow, Cal Tech. Hyp. Res. Proj., GALCIT Memo No. 58 (1960).
8. S. Ziering, Shear and heat flow for maxwellian molecules, *Physics of Fluids* **5**, 275–279 (1962).
9. D. J. Alofs, R. C. Flagan and G. S. Springer, Density distribution measurements in rarefied gases contained between parallel plates at high temperature differences, *Physics of Fluids* **14**, 529–533 (1969).
10. C. Y. Liu and L. Lees, Plane Compressible Couette Flow, *Rarefied Gas Dynamics*, L. Talbot, ed., Academic Press, New York, 391–428 (1961).
11. G. A. Bird, Aspects of the structure of strong shock waves, *Physics Fluids* **13**, 1172–1177 (1970).
12. S. M. Yen, *et al.*, Solutions of the non-linear Boltzmann equation for shock waves in a Maxwellian gas, (in press).
13. H. M. Mott-Smith, Solution of Boltzmann equation for a shock wave, *Phys. Rev.* **82**, 885–892 (1951).
14. G. A. Bird, Breakdown of translational and rotational equilibrium in gaseous expansions, *AIAA J.* **8**, 1998–2003 (1970).
15. A. H. Shapiro, *The Dynamics and Thermodynamics of Compressible Fluid Flow*, **1**, Ronald, New York (1953).
16. T. Soga and H. Oguchi, Numerical analysis on source expansion flow into vacuum, *Physics of Fluids* **15**, 766–771 (1972).
17. B. B. Hamel, and D. R. Willis, Kinetic theory of source flow expansions with application to the free jet, *Physics of Fluids* **9**, 829–841 (1966).
18. S. M. Yen, Monte Carlo solutions of nonlinear Boltzmann equation for problems of heat transfer in rarefied gases, *Int. J. Heat Mass Transfer* **14**, 1865–1869 (1971).
19. B. L. Hicks and S. M. Yen, Solution of the non-linear Boltzmann equation for plane shock waves, *Rarefied Gas Dynamics*, L. Trilling and H. Y. Wachman, ed. **1**, Academic Press, New York (1969).